Kovove Mater. 51 2013 211–220
DOI: 10.4149/km_2013_4_211

Newton thermal analysis of unmodified and strontium modified Al-Si alloys

R. Aparicio[1], C. Gonzalez-Rivera[2]*, M. Ramirez-Argaez[2], G. Barrera[3], G. Trapaga[1]

[1] *CINVESTAV Querétaro, Libramiento Norponiente 2000, Real de Juriquilla, 76230 Querétaro Qro., México*
[2] *Departamento de Ingeniería Metalúrgica, Facultad de Química, Universidad Nacional Autónoma de México, Edificio D Av. Universidad 3000, 04510 México D. F., México*
[3] *Instituto de Investigaciones Metalúrgicas, UMSNH, Apdo. postal 888 Centro, 58000, Morelia Mich., México*

Received 18 October 2011, received in revised form 24 October 2012, accepted 26 October 2012

Abstract

The aim of this work was to explore changes in the solidification kinetics associated with the presence of modified and nonmodified Al-Si eutectic in Al-Si alloys, as revealed by Newton thermal analysis (NTA). Hypoeutectic and near eutectic Al-Si melts with different Sr contents were produced in silicon carbide crucibles. The addition of strontium to the melts was accomplished using a Al-10%Sr master alloy. The chemical composition was controlled by spark emission spectrometry. Microstructural characterization of experimental probes was performed by optical microscopy. NTA was carried out at two different cooling rate conditions using a type K thermocouple. NTA results show that an increase in Sr content produces changes in solidification rate evolution at the beginning of eutectic solidification of the experimental alloys. During the rest of solidification, both modified and unmodified eutectic show similar solidification rate evolution.

K e y w o r d s: solidification kinetics, Al-Si, undercooling, eutectic modification

1. Introduction

Modification of as-cast Al-Si alloys by chemical additions is a well-known industrial practice employed to transform the eutectic silicon phase from a coarse plate or flake-like structure to a fine fibrous structure, thereby improving mechanical properties of the castings. The fine fibrous eutectic modification of hypoeutectic Al-Si alloys that occurs when elements such as strontium and sodium are added has been explained on the basis of observations of increased twinning [1]. The increased density of twinning is believed to result from an impurity-induced twinning (IIT) mechanism that promotes further growth by encouraging the formation of a perpetuating twin plane re-entrant edge (TPRE) [2, 3].

More recently, modification has been found to change the nucleation frequency and dynamics of eutectic grains with the associated effects on the growth rate [4]. The mechanism of modification is probably related both to reduction in nucleation frequency of eutectic grains and to changing growth by IIT [5], however, it is still not fully understood.

Given that eutectic Al-Si modification mechanisms have been explained in terms of changes in nucleation and growth kinetics of silicon, it is interesting to explore the effect of additions of modifying elements on solidification kinetics and eutectic morphology of Al-Si alloys as revealed by computer aided cooling curve analysis (CA-CCA).

Numerical processing of cooling curves using CA-CCA can be used to generate information on solidification kinetics. The simplest CA-CCA method is Newton thermal analysis (NTA), which assumes absence of thermal gradients in the sample during cooling process. The NTA methodology has been described in detail elsewhere [6, 7]. Briefly, a cooling curve obtained with a thermocouple located at the thermal center of a liquid cast is analyzed. NTA numerical processing starts with the generation of the first derivative with respect to time of this curve. After calculation of the derivative, the points corresponding to the start and

*Corresponding author: carlosgr@unam.mx

Table 1. Chemical composition of the experimental melts prior to Sr modification

Alloy	Si	Fe	Cu	Mn	Mg	Ti	Sr	Al
A356	6.6	0.36	0.02	0.05	0.33	0.01	0.0002	Bal
Eutectic	12.4	0.34	0.02	0.05	0.30	0.017	0.0002	Bal

the end of solidification are identified and the zero baseline curve is obtained from an exponential interpolation between these points. The integration of the area between the first derivative of the cooling curve and the zero baseline curves gives relevant quantitative information on solidification kinetics.

It has been argued that the NTA method is not reliable for making quantitative predictions of latent heat of solidification due to the arbitrary nature of the zero curve calculation [7, 8], however, it has potential as an approximate, semi quantitative method to study the solidification kinetics of several cases of metallurgical interest [9–12]. The NTA method shows also a good potential as a tool for detecting changes in solidification kinetics, i.e., the evolution of solid fraction and its derivative with respect to time, the latter parameter known as solidification rate, in the presence of different solidification mechanisms during solid formation [12].

The eutectic Al-Si modification with Sr is accompanied by a large increase in undercooling of the eutectic arrest. It is well known that, during solidification from undercooled metallic melts, an increase in cooling rate refines the microstructure as a result of the effect of the presence of more undercooling on the nucleation and growth of the solidification products.

Taking into account that both the chemical modification of the eutectic and the increase in cooling rate produce changes in the solidification conditions affecting the kinetics of solid formation, the aim of this work was to explore the effect of Sr modification and cooling rate on the solidification kinetics of a hypoeutectic and a near-eutectic Al-Si alloys using NTA.

2. Experimental

In order to obtain two liquid Al-Si based alloys with Si contents typical of a hypoeutectic (A356) alloy and a nearly eutectic (Al-12%Si) alloy, melts were produced in a SiC crucible in an electric furnace with an argon atmosphere using burdens of A356 alloy and commercial purity silicon. Table 1 shows the chemical composition of the experimental melts. The addition of strontium was made using Al-10wt.%Sr master alloy. For hypoeutectic alloys, strontium addition levels were in the range of 0 to 150 ppm, while for near-eutectic alloys the range was from 0 to 200 ppm. The chemical composition was adjusted by spark emission spectroscopy.

Thermal analysis test samples were taken by submerging into the melt a cylindrical stainless steel test crucible (0.03 m inner diameter, 0.05 m in height, and 0.0015 m in thickness, covered with boron nitride). The crucibles were kept submerged for approximately 30 s, so that they could reach the bath temperature. Next, they were removed from the melt and placed on the thermal analysis test stand, where they were thermally isolated at the top and bottom. In this stand, and in order to record the thermal history of the alloy during cooling, a 0.0003 m diameter bore, type K thermocouple with alumina two bore insulator, 0.0015 m OD, was introduced at the mid-height of the mold cavity at the center of the probe. The thermocouple output was converted from analog to digital by means of a data acquisition card, NI FieldPoint cFP 1804, and recorded into a PC hard disk drive, for a numerical post-processing task. A compressed air ring was used to study the effect of a high cooling rate on cooling curves, microstructure and solidification kinetics characterization of experimental probes. The air ring was surrounding the mold containing the sample. To perform experiments at a high level of cooling rate, a flow of $77\,\mathrm{l\,min^{-1}}$ of air was used. For the low cooling rate condition, natural convection air cooling was allowed. A calibration procedure was performed with 99.9 % aluminum. The experimental cooling curves were numerically processed using the NTA method to obtain information about the evolution of solid fraction during solidification of the sample.

For microstructural analysis, the samples were transversely sectioned and prepared by standard polishing procedures. The microstructure of the specimens was observed by optical microscopy.

3. Results and discussion

Typical results of the effect of an increase in Sr content on the cooling curves, microstructure, and solidification kinetics of hypoeutectic A356 Al-Si alloy probes are shown in Figs. 1–3.

Figure 1 presents the effect of Sr content on the cooling curves of the hypoeutectic alloy under low cooling rate conditions. Temperature evolution during cooling and solidification of commercial hypoeutectic Al-Si alloys comprises four main stages: (1) Cooling of the liquid from the beginning of cooling process to the start of primary solidification; (2) Solidification of dendrites of primary phase; (3) Solidification

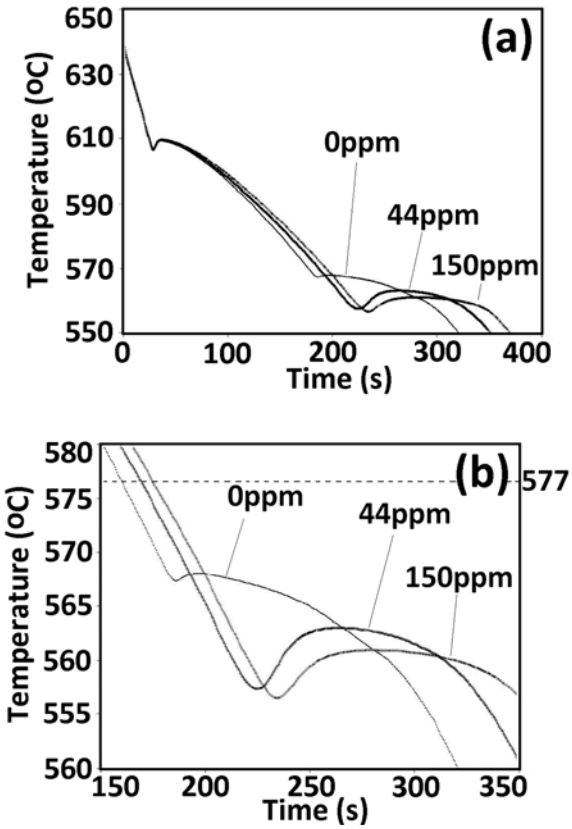

Fig. 1. Effect of Sr content on cooling curves of the hypoeutectic alloy under low cooling rate conditions: (a) cooling curves and (b) detail of curves during eutectic solidification.

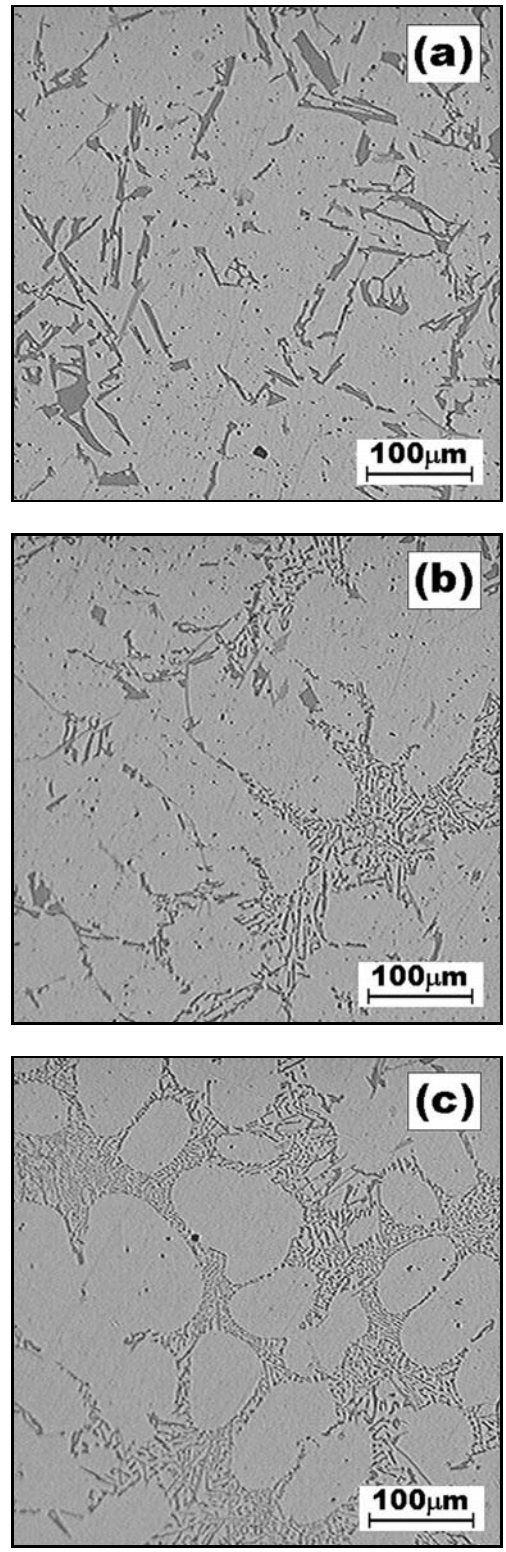

Fig. 2. Effect of Sr content on the microstructure of the hypoeutectic alloy solidified at low cooling rate: (a) 0 ppm Sr, (b) 44 ppm Sr, and (c) 150 ppm Sr.

of eutectic constituent until the reaching the end of solidification, and (4) Cooling of the solid. Accordingly, there are two plateaus on each cooling curve, corresponding to the solidification and latent heat release of the two main microconstituents of A356 alloy: dendrites of Al-rich primary phase and eutectic microconstituent. In Fig. 2, these phases appear respectively as the bright and dark microconstituents, and a detailed inspection of those micrographs permits to see, as expected, that an increase in Sr content promotes the modification of the eutectic microconstituent.

Back to Fig. 1, for the three Sr levels cooling curves are almost identical during cooling of the liquid and primary phase solidification stages, but there are important differences during eutectic solidification, indicating that Sr presence affects mainly the eutectic constituent. Figure 1b shows in more detail the stage of eutectic solidification, where it can be seen that an increase in Sr content produces an increase in the operating undercooling during eutectic solidification, defined as the difference between equilibrium Al-Si eutectic temperature (577 ℃) and the actual temperature measured during eutectic nucleation and growth.

Three characteristic temperatures were measured for the eutectic reaction detected on the cooling curves. These temperatures were the nucleation tem-

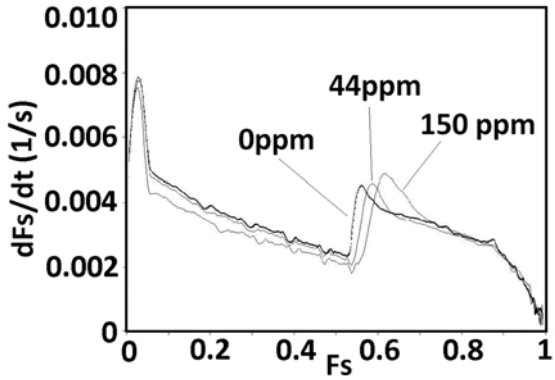

Fig. 3. Effect of Sr content on NTA solidification kinetics of hypoeutectic alloy.

Table 2. Characteristic temperatures (nucleation, minimum and growth) for the eutectic reactions of the cooling curves shown in Fig. 1

Sr content (ppm)	T_N (℃)	T_M (℃)	T_G (℃)
0	569.9	567.7	568.4
44	560.8	556.9	562.6
150	560.2	556.4	560.9

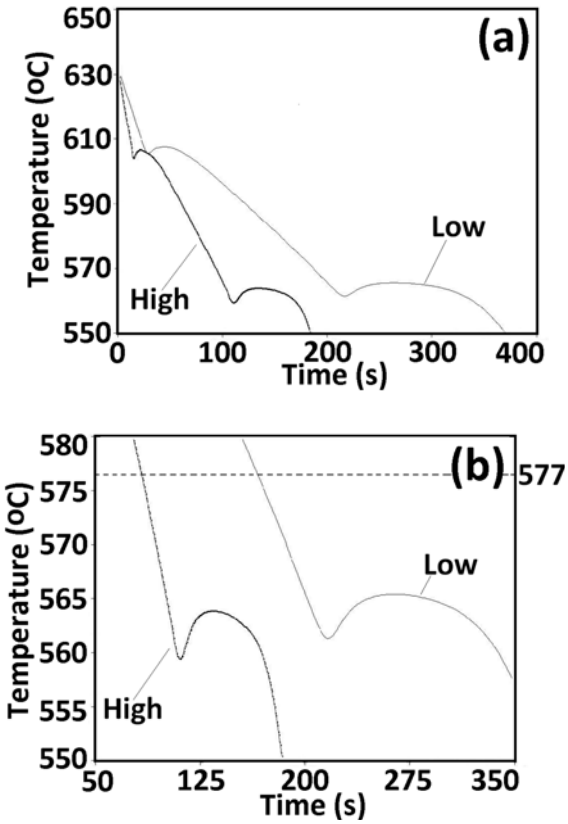

Fig. 4. Effect of cooling rate on (a) cooling curves and (b) detail of curves during eutectic formation for A356 with 150 ppm Sr.

perature, T_N, defined as the first noticeable change on the derivative of the cooling curve; the minimum temperature prior to recalescence, T_M, and the growth temperature, T_G, defined as the maximum reaction temperature reached after recalescence [13].

Table 2 displays the characteristic temperatures for eutectic solidification of the curves shown in Fig. 1. As expected, strontium additions to the unmodified commercial alloy caused a reduction of the three characteristic temperatures, pointing out to the presence of a higher operating undercooling during eutectic solidification of Sr modified alloys.

Solidification kinetics is commonly represented by a plot of solid rate formation against solid fraction, which allows analyzing solidification rate evolution as the microconstituents nucleate and grow. Figure 3 presents solidification kinetics obtained from the NTA numerical processing of the cooling curves shown in Fig. 1. Two maxima are associated with the two main microconstituents formed during solidification of the experimental alloys. The first maximum corresponds to dendrites of primary phase and the second maximum to the eutectic constituent.

Figure 3 shows also the effect of changes in Sr content on NTA solidification kinetics in probes solidified at low cooling rates. The NTA method permits to see changes of solidification rate only at the beginning of eutectic solidification, which indicates that an increase in Sr content causes a delay in the start of eutectic formation and an increase in solid formation rate at the first moments of eutectic solidification, i.e., during its nucleation. It is noteworthy that after eutectic nucleation, probes show similar eutectic formation rate despite the differences in operating undercooling during its growth, Fig. 1b, Table 2.

As for the effect of cooling rate on cooling curves, microstructure, and solidification kinetics of hypo eutectic Al-Si alloys with a specific Sr content, Fig. 4a shows the cooling curves associated with the cooling and solidification of the hypoeutectic alloy with 150 ppm Sr under low and high cooling rate conditions. Figure 4b presents in more detail the region of the curves corresponding to the solidification of eutectic microconstituent. The broken horizontal line shows the equilibrium Al-Si eutectic temperature of 577℃. As seen in this figure, an increase in cooling rate, under the experimental conditions of this work, increases the operating eutectic undercooling, reaching similar values to undercooling caused by Sr addition, Fig. 1b. Table 3 displays the characteristic temperatures measured on the cooling curves shown in Fig. 4a for primary dendrites and eutectic microconstituent.

A higher cooling rate promotes the decrease of T_N,

Table 3. Characteristic temperatures (nucleation, minimum and growth) for the primary and eutectic reactions observed on the cooling curves shown in Fig. 4

Cooling rate	Microconstituent	T_N (℃)	T_M (℃)	T_G (℃)
Low	Primary Al	612.8	605.1	607.1
Low	Al-Si eutectic	562.9	560.8	565.1
High	Primary Al	608.3	603.9	606.1
High	Al-Si eutectic	560.8	558.8	563.4

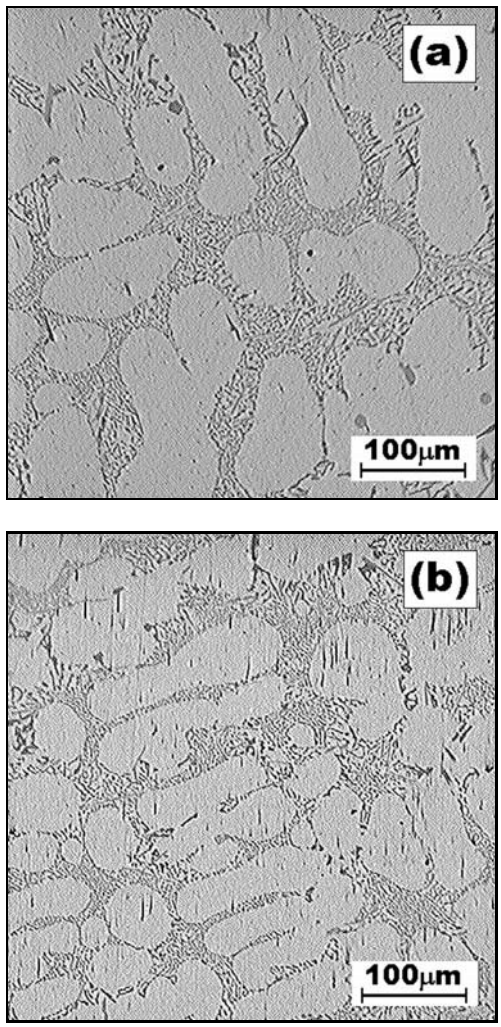

Fig. 5. Effect of cooling rate on microstructure of the hypoeutectic alloy with 150 ppm Sr: (a) low cooling rate and (b) high cooling rate.

T_M and T_G for both primary and eutectic microconstituents and at the same time increases acting undercooling during solidification of both microconstituents which in turn produces the refinement of these microconstituents as observed in the micrographs of Fig. 5.

Figure 6 shows solidification kinetics obtained from the NTA numerical processing of the cooling curves shown in Fig. 4. A rise in the cooling rate from the low to the high cooling rate condition causes an increase of the solidification rate of almost twofold the values obtained for low cooling rate. Results presented in Figs. 4 to 6 suggest that an increase in cooling rate promotes higher operating undercooling during solidification, increasing solidification rate formation and refining microstructure.

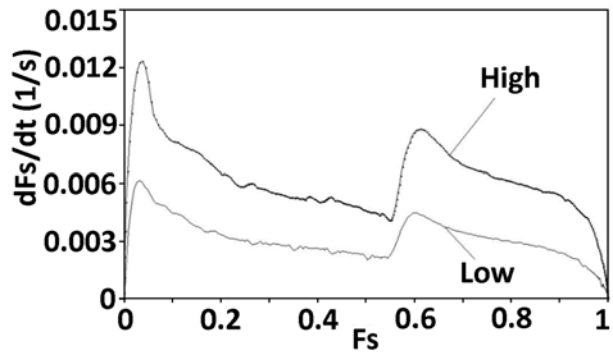

Fig. 6. Effect of cooling rate on NTA solidification kinetics of the hypoeutectic alloy with 150 ppm Sr.

Figure 7 presents the effect of Sr content and cooling rate on NTA solidification kinetics of the hypoeutectic alloy. For the two cooling conditions, the same trends appear concerning the effect of a rise in Sr content on solidification kinetics, including a rise in solidification rate during the first moments, i.e., during nucleation, of eutectic solidification and an increase in the amount of primary phase formed during solidification. This suggests an increase of kinetic barriers affecting eutectic nucleation as a result of the presence of Sr. It also can be noticed that after the initial stage of eutectic nucleation, solidification rates are similar for samples solidified at the same cooling rate, despite differences in operating eutectic undercooling for modified and non-modified samples.

Similar results were obtained for the solidification kinetics characterization of the near-eutectic alloy studied in this work, solidified under different conditions of Sr content and cooling rate. Typical results of the effect of an increase in cooling rate on cooling curves, microstructure, and solidification kinetics of nearly eutectic alloy probes with a specific level of Sr are shown in Figs. 8–10.

Figure 8a presents the cooling curves corresponding to the two experimental cooling conditions for

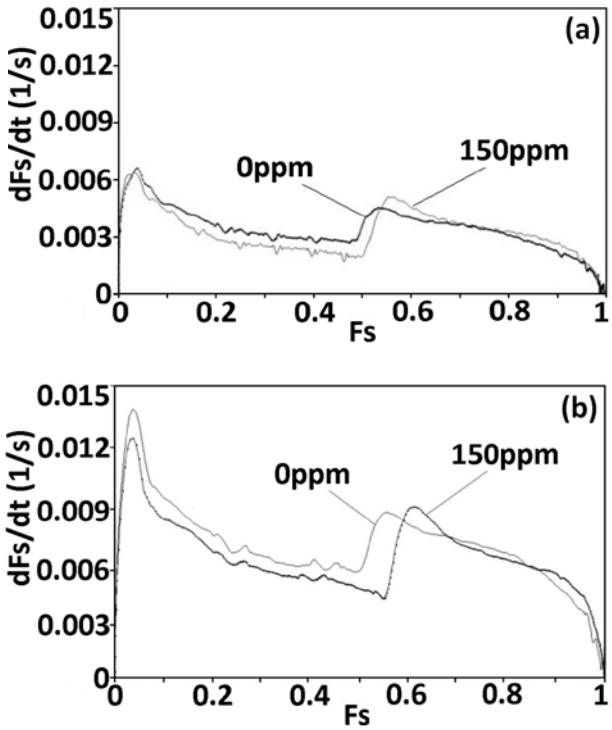

Fig. 7. Effect of Sr content and cooling rate on NTA solidification kinetics of the hypoeutectic alloy: (a) low cooling rate and (b) high cooling rate.

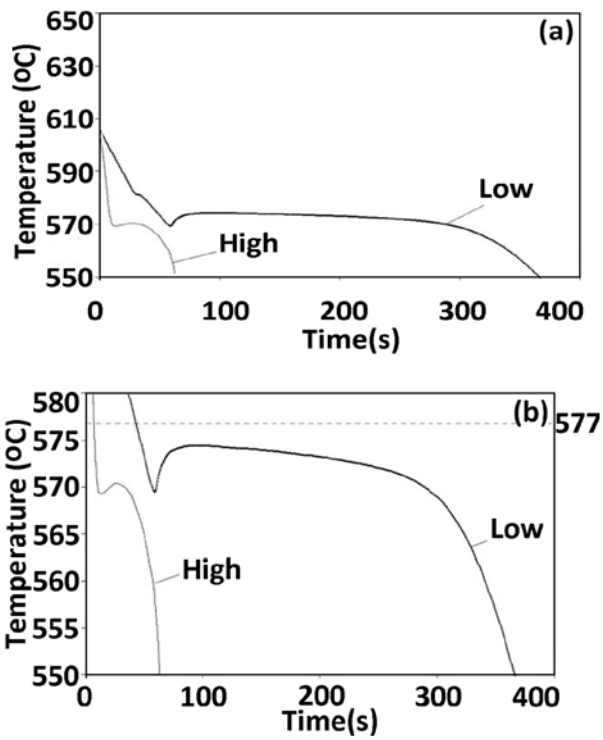

Fig. 8. Effect of cooling rate on the cooling curves for the near-eutectic Al-Si alloy without Sr: (a) cooling curves and (b) detail of curves during eutectic solidification.

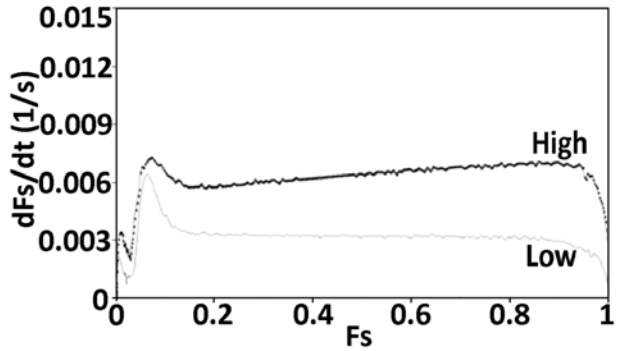

Fig. 9. Effect of cooling rate on the NTA solidification rate for the near-eutectic Al-Si alloy without Sr.

the near-eutectic alloy without Sr. On each cooling curve there is a first stage of cooling of the liquid, shown as the continuous drop in temperature from the beginning of the measurement, followed, as the curve approaches eutectic temperature, by a very slight decrease in slope corresponding to solidification of primary silicon and almost immediately after, by the presence of a plateau corresponding to the solidification of the main, eutectic, microconstituent. Finally, after the eutectic plateau, temperature drops again, in the final stage of cooling of the solid alloy. A higher cooling rate reduces the time needed by the probe to reach a given temperature, which appears more clearly in this figure as the increase, with reference to the cooling curve obtained at low cooling rate, of the slopes of the cooling curve at high cooling rate during the initial and final stages of cooling.

Figure 8b shows in more detail the cooling curves during eutectic solidification. The dotted line represents the equilibrium Al-Si eutectic temperature. It can be noted that an increase in cooling rate decreases operating temperatures present during solidification; also operating eutectic undercooling increases as a result of a higher cooling rate. This increase in undercooling produces an increase in the solidification rate (Fig. 9) and a refinement of the microstructure (Fig. 10).

Figure 9 presents the solidification rate evolution of the near eutectic alloy during its solidification under the two cooling conditions as predicted by the NTA processing of the curves shown in Fig. 8. A first maximum is observed on these curves, at the beginning of solidification, which apparently corresponds to nucleation and growth of primary silicon, followed by a second maximum and a relatively flat plateau associated with nucleation and growth of eutectic constituent. The NTA processing of the experimental cooling curves shows an increase in solidification rate as a result of the increase in cooling rate. Under the experimental conditions of this work, there is an almost twofold increase in solidification rate during eutectic

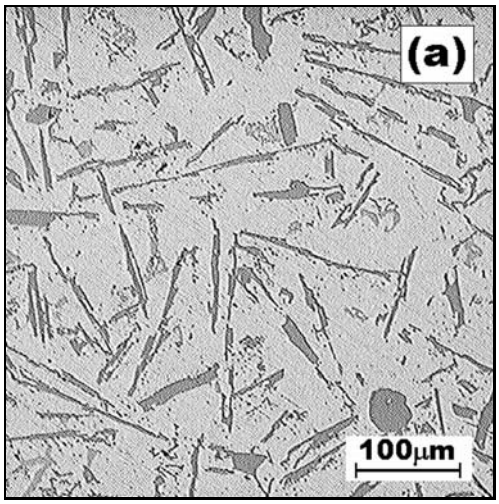

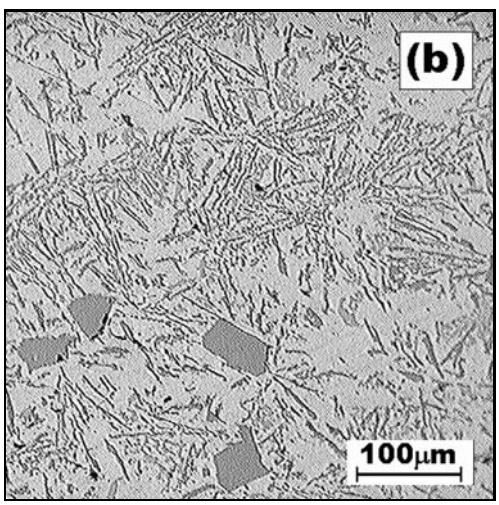

Fig. 10. Effect of cooling rate on microstructure of the near-eutectic Al-Si alloy without Sr: (a) low cooling rate and (b) high cooling rate.

growth of the probe solidified under the high cooling rate compared with the low rate condition.

Figure 10 shows microstructures of the near eutectic alloy without Sr solidified under the two cooling conditions. In both cases, it is noticeable the presence of primary silicon polyhedral crystals embedded in an eutectic Al-Si, showing a coarse plate-like silicon morphology typical of Al-Si alloys without modification treatment. In some cases, silicon flakes radiate

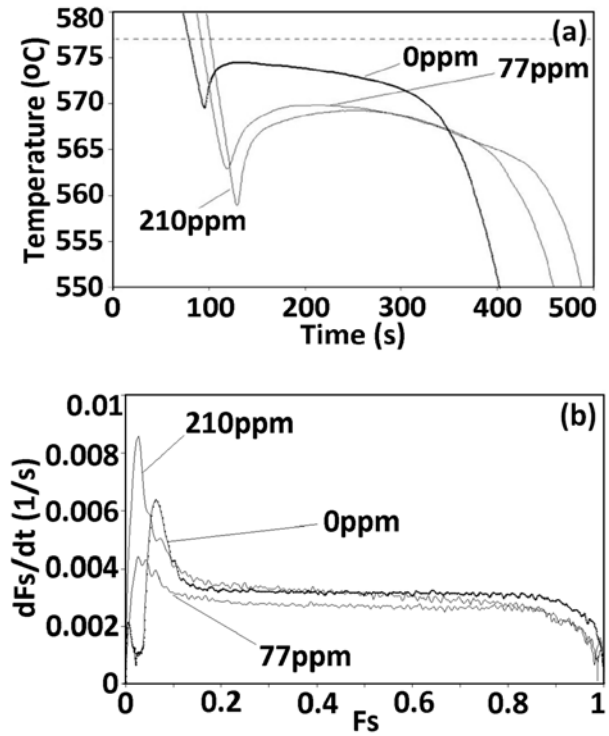

Fig. 11a,b. Effect of Sr content on cooling curves and solidification kinetics of the near-eutetic alloy under low cooling rate conditions.

from silicon crystals. Comparing the microstructures, it can be seen that an increase in cooling rate under our experimental conditions causes the refinement of microstructure.

Results presented in Figs. 8 to 10 suggest that an increase in cooling rate promotes higher operating undercooling during solidification, which in turn increases solidification rate formation and refines the microstructure.

Figure 11a shows the effect of Sr content on the cooling curves of the near-eutectic alloy. An increase in Sr content reduces the temperatures present during eutectic solidification; the operating eutectic undercooling increases and reaches values similar or even higher than those caused by a change in cooling rate (Fig. 8b). Table 4 displays characteristic eutectic temperatures of the cooling curves shown in Figs. 8b and 11a.

Table 4. Characteristic temperatures (nucleation, minimum and growth) for the eutectic reactions observed on the cooling curves shown in Figs. 9b and 11a

Cooling rate	Sr content (ppm)	T_N (℃)	T_M (℃)	T_G (℃)
Low	0	570.6	569.3	574.4
High	0	570.3	569.2	570.4
Low	77	566.7	562.8	569.8
Low	210	560.9	558.8	569.2

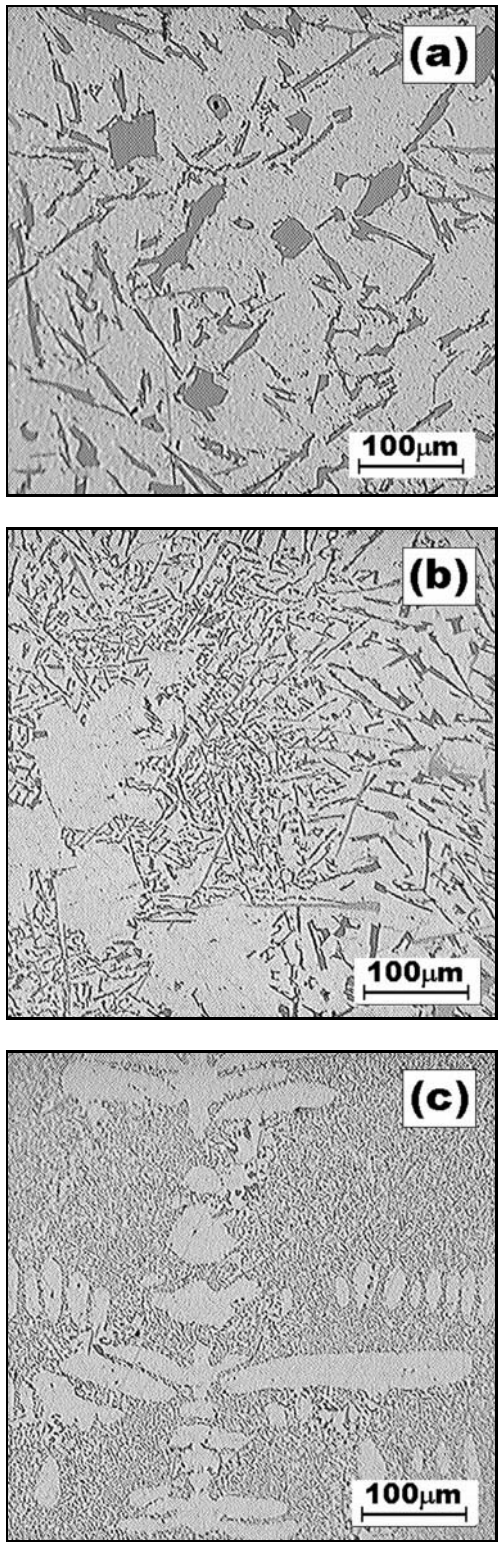

Fig. 12. Effect of Sr content on microstructure of the near-eutectic Al-Si alloy at low cooling rate: (a) 0 ppm Sr, (b) 78 ppm Sr and (c) 210 ppm Sr.

Data in Table 4 indicate that an increase in cooling rate for the strontium-free alloy causes an increase in operating undercooling during solidification comparable to the change that results from the presence of Sr causing eutectic modification.

Figure 11b presents the solidification kinetics obtained from numerical processing of cooling curves shown in Fig. 11a. Results in Fig. 11b reveal important differences between solidification rate evolution of experimental probes at the beginning of solidification, and similar solidification rate evolution during the rest of solidification. The first maximum, originally present in the Sr free alloy, disappears, as Sr content is raised apparently as a result of the action of Sr, which poisons the nucleation sites for primary silicon. This can be inferred from the microstructural results found for the probes containing 77 and 210 ppm of Sr. In these probes, primary silicon polyhedral crystals have been practically eliminated (Fig. 12) as a result of Sr additions.

In this regard, it has been proposed [13] that Sr neutralizes the phosphorus-based nucleants commonly present in the unmodified alloys through the formation of Sr-rich intermetallics in AlP nucleant particles [14].

The rise in the first maximum present in the solidification rate evolution of the eutectic alloys with 77 and 210 ppm of Sr (Fig. 11b) may be associated with the increase in eutectic nucleation barriers as Sr content is increased and also as a result of the increased occurrence of primary aluminum dendrites that can develop more easily under the restrictions imposed for eutectic nucleation in presence of Sr.

In Fig. 11b, it can be noticed that after the initial stage of solidification, i.e., for solid fractions higher than 0.2, solidification rates for modified and unmodified Al-Si eutectic are similar despite differences in operating eutectic undercooling (Fig. 11a, Table 4).

Figure 12 shows that an increase in Sr content has eliminated silicon primary crystals originally present in the Sr-free eutectic alloy promoting the gradual modification of the eutectic.

The experimental results show that, after the initial stage of nucleation, there are similar paths in the solidification rate evolution for the eutectic in both the hypoeutectic and the near-eutectic alloy, modified or not with Sr under the same cooling conditions. This result suggests that under the same conditions of rate of heat extraction, the rate of latent heat production is apparently the same. Equation (1) shows a lumped energy balance of the system under study. This balance is the foundation of the NTA method.

$$qA + L_{\mathrm{f}}\mathrm{d}F_{\mathrm{s}}/\mathrm{d}t = mC_{\mathrm{p}}\mathrm{d}T/\mathrm{d}t. \qquad (1)$$

In Eq. (1), q is the heat flux leaving the sample, A is the thermal exchange area, L_{f} is the latent heat of solidification that can be released by the sample, $\mathrm{d}F_{\mathrm{s}}/\mathrm{d}t$ is the solidification rate, and m and C_{p} are the mass and the heat capacity of the sample, respect-

ively. The first term of Eq. (1) represents the heat flow leaving the sample through the thermal exchange area A. The second term is the latent heat flow released by the sample which solidifies at a solidification rate $\mathrm{d}F_\mathrm{s}/\mathrm{d}t$, and the third term is the rate of change of the enthalpy of the sample. The NTA results show that $\mathrm{d}F_\mathrm{s}/\mathrm{d}t$ evolution depends mainly on the heat flow leaving the sample despite the difference in operating undercoolings in modified and non-modified probes cooled at the same cooling rate.

In order to be able to discuss why this happens despite the presence of different undercoolings, it has to be found a relationship connecting the solidification rate and the undercooling. For a simple model of equiaxed eutectic growth involving the growth of N spheres of the same radius, where N is the grain density, the following equations can be applied:

$$\mathrm{d}F_\mathrm{s}/\mathrm{d}t = 4\pi N R^2 \mathrm{d}R/\mathrm{d}t f_\mathrm{i}, \tag{2}$$

$$\mathrm{d}R/\mathrm{d}t = \mu \Delta T^n. \tag{3}$$

In Eq. (2), R is the instantaneous grain radius, $\mathrm{d}R/\mathrm{d}t$ is the grain growth rate which has been represented as an exponential function of ΔT, the undercooling (see Eq. (3)), where μ and n are the pre-exponential and the exponential growth coefficients, respectively. In Eq. (2), f_i is a factor that introduces the effect of the impingement of growing grains at the end of solidification.

It has been found that the eutectic Al-Si grain density is decreased notoriously as a result of the presence of Sr, and it could be expected a difference between the N values in Eq. (1) corresponding to non-modified and Sr-modified Al-Si eutectic. For instance, for Al-10%Si alloys it has been found [15] that an increase of 100 ppm of Sr reduces in two orders of magnitude the number of grains by unit area. The second difference that could be expected when comparing the undercoolings present during solidification of modified and non-modified eutectic, is the grain growth rate. The observed similarity of solidification rate could be explained by changing the values of the pre-exponential and exponential coefficients describing the dependence of grain growth rate on the undercooling. This change could be associated to the change in the growth mechanism of the eutectic in both conditions. Indeed Degand [16], who performed experiments with undercooled Al-Si eutectic alloy, has found that, maintaining the value of the exponential coefficient to $n = 2$ in Eq. (3), according to the classical theory of eutectic growth, the presence of Sr decreases the value of the pre-exponential growth coefficient.

The change in these coefficients could be related to the nature of the causes that change the undercooling. For solidification in undercooled melts, the total undercooling at the solid/liquid interface with respect to the bulk temperature is made of the algebraic sum of several contributions [17], as is shown in Eq. (4), where the left hand side term, ΔT, is the total undercooling, ΔT_k is the kinetic undercooling, ΔT_r is the interfacial undercooling, ΔT_c is the constitutional undercooling, and ΔT_t is the thermal undercooling.

$$\Delta T = \Delta T_\mathrm{t} + \Delta T_\mathrm{c} + \Delta T_\mathrm{r} + \Delta T_\mathrm{k}. \tag{4}$$

Apparently, when the total undercooling is increased as a result of a bigger rate of heat extraction, the increase is due to the rise of the thermal undercooling, with a direct consequence on the solidification rate, as can be seen in Figs. 6 and 9.

On the other hand, the increase in undercooling, resulting from the Sr additions to the experimental melts, could be the result of changes in ΔT_k, taking into account that Sr locates preferentially on the surfaces of the growing silicon of the eutectic [18], ΔT_r, that could be affected as a result of the change in morphology of the eutectic, and ΔT_c as a result of the possible changes in solute distribution associated with the two effects mentioned above. The increase in total undercooling due to those factors does not contribute apparently to a change in solidification rate which is apparently governed by the heat extraction conditions during solidification.

The NTA results apparently support this affirmation showing that the increase of total undercooling in presence of more Sr does not produce an increase in solid rate formation. Finally, NTA results suggest that Sr modification of eutectic causes a change in the mechanism operating during Al-Si eutectic solidification. The observed behavior could be explained as a result of two different growth mechanisms operating during eutectic solidification of Sr modified and unmodified Al-Si eutectic, each one with its own dependence between solidification kinetics and operating undercooling.

4. Conclusions

The eutectic modification with Sr produces changes in the solidification kinetics revealed by the NTA method for the hypoeutectic and the near-eutectic Al-Si alloys studied in this work.

For the hypoeutectic alloy, NTA results indicate, for samples solidified at the same cooling rate, that an increase in Sr content causes a delay in the start of eutectic formation and an increase in solid formation rate at the first moments of eutectic solidification. After this initial stage of eutectic solidification, the modified and unmodified probes show similar eutectic solidification rate evolution.

The same trend is observed for the near-eutectic alloy. An increase in Sr content brings about changes

in solidification rate evolution at the beginning of solidification that may be associated with changes in eutectic nucleation, as suggested by microstructural findings showing the elimination of originally present primary silicon crystals due to Sr additions. During the rest of solidification, both modified and unmodified eutectics show similar solidification rate evolution, which suggests that this parameter is governed mainly by the rate of heat extraction.

For all the probes, an increase in cooling rate under experimental conditions shows an almost twofold increase in solidification rate for the probe solidified under the high cooling rate compared with the low rate condition.

For the same cooling rate conditions, the observed increase in operating undercooling caused by Sr additions apparently did not produce changes in solidification rate compared with the Sr-free alloy during growth of the eutectic, after the eutectic nucleation stage. This effect could be related to the different solidification mechanisms acting during growth of modified and unmodified Al-Si eutectic, each one with its own dependence between solidification kinetics and operating undercooling.

Acknowledgements

R. Aparicio and C. Gonzalez-Rivera acknowledge CONACYT Mexico for its support through student and sabbatical grants, respectively.

C. Gonzalez acknowledges the DGAPA UNAM for its financial support (Project IN113912).

All the authors acknowledge A. Ruiz, A. Amaro, C. Atlatenco, A. Galindo and I. Beltran for their valuable technical assistance and to CINVESTAV Queretaro, IPN and CONCYTEQ for an additional support.

References

[1] Nogita, K., Yasudab, H., Yoshiya, M., McDonald, S. D., Uesugi, K., Takeuchi, A., Suzuki, Y.: J. Alloy Compd., *489*, 2010, p. 415. doi:10.1016/j.jallcom.2009.09.138

[2] Lu, S. Z., Hellawell, A.: Metall. Trans. A, *18A*, 1987, p. 1721.

[3] Gruzleski, J. E., Glosset, B. M.: The Treatment of Liquid Aluminum-Silicon Alloys. Des Plaines, Illinois, AFS 1990.

[4] Dahle, A. K., Nogita, K., Zindel, J. W., McDonald, S. D., Hogan L. M.: Metall. Mater. Trans. A, *32A*, 2001, p. 949. doi:10.1007/s11661-001-0352-y

[5] Cho, Y. H., Dahle, A. K.: Metall. Mater. Trans. A, *40A*, 2009, p. 1011. doi:10.1007/s11661-009-9820-6

[6] Upadhya, K. G., Stefanescu, D. M., Lieu, K., Yeager, D. P.: AFS Trans., *97*, 1989, p. 61.

[7] Barlow, J. O., Stefanescu, D. M.: AFS Trans., *105*, 1997, p. 349.

[8] Emadi, D., Whiting, L. V.: AFS Trans., *110*, 2002, p. 285.

[9] Mac Kay, R. J., Djurdjevic, M. B., Sokolowsky, J. H.: AFS Trans., *108*, 2000, p. 521.

[10] Oliveira, M., Malheiros, L., Ribeiro, C. A.: J. Mater. Proces. Tech., *92–93*, 1999, p. 25. doi:10.1016/S0924-0136(99)00181-8

[11] González-Rivera, C., Baez, J., Chavez, R., Alvarez, O., Juarez-Islas, J.: Int. J. Cast Metal. Res., *16*, 2003, p. 531.

[12] Chavez, M. R., Amaro, A., Flores, C., Juarez, A., González-Rivera, C.: Mater. Sci. Forum, *509*, 2006, p. 153. doi:10.4028/www.scientific.net/MSF.509.153

[13] McDonald, S. D., Nogita, K., Dahle, A. K.: Acta Mater., *52*, 2004, p. 4273. doi:10.1016/j.actamat.2004.05.043

[14] Cho, Y. H., Lee, H. C., Oh, K. H., Dahle, A. K.: Metall. Mater. Trans. A, *39A*, 2008, p. 2435. doi:10.1007/s11661-008-9580-8

[15] McDonald, S. D., Dahle, A. K., Taylor, J. A., Stjohn, D. H.: Metall. Mater. Trans. A, *35A*, 2004, p. 1829. doi:10.1007/s11661-004-0091-y

[16] Degand, C., Stefanescu, D. M., Laslaz, G.: In: Solidification Science and Processing. Eds.: Ohnaba, I., Stefanescu, D. M., Warrendale, T. M. S. 1996, p. 55.

[17] Stefanescu, D. M.: Science and Engineering of Casting Solidification. 2nd Ed. New York, Springer Science 2009.

[18] McDonald, S. D., Tsujimoto K., Yasuda, K., Dahle, A. K.: J. of Electron Microscopy, *53*, 2004, p. 361.